ERDC/CRREL TR-17-2

Cold Regions Research and Engineering Laboratory

US Army Corps of Engineers®
Engineer Research and Development Center

ERDC
INNOVATIVE SOLUTIONS for a safer, better world

Engineering for Polar Operations, Logistics, and Research (EPOLAR)

Geophysical Survey of McMurdo Ice Shelf to Determine Infrastructure Stability and for Future Planning

Seth Campbell, Zoe Courville, Samantha Sinclair, and Joel Wilner

January 2017

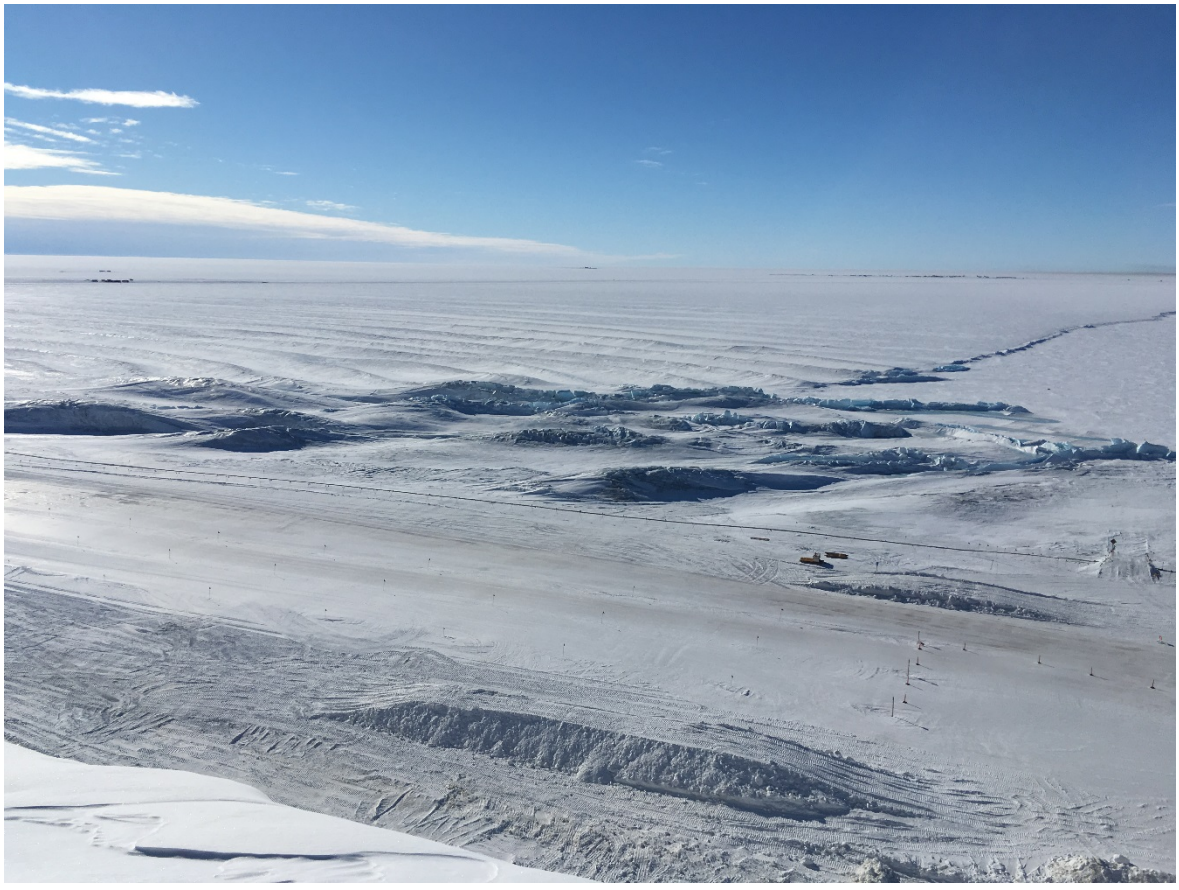

The U.S. Army Engineer Research and Development Center (ERDC) solves the nation's toughest engineering and environmental challenges. ERDC develops innovative solutions in civil and military engineering, geospatial sciences, water resources, and environmental sciences for the Army, the Department of Defense, civilian agencies, and our nation's public good. Find out more at www.erdc.usace.army.mil.

To search for other technical reports published by ERDC, visit the ERDC online library at http://acwc.sdp.sirsi.net/client/default.

ERDC/CRREL TR-17-2
January 2017

Geophysical Survey of McMurdo Ice Shelf to Determine Infrastructure Stability and for Future Planning

Seth Campbell, Zoe Courville, and Samantha Sinclair

U.S. Army Engineer Research and Development Center (ERDC)
Cold Regions Research and Engineering Laboratory (CRREL)
72 Lyme Road
Hanover, NH 03755-1290

Joel Wilner

Department of Geology
McCardell Bicentennial Hall
276 Bicentennial Way
Middlebury College
Middlebury, VT 05753

Final Report

Prepared for National Science Foundation, Office of Polar Programs,
Antarctic Infrastructure and Logistics
Arlington, VA 22230

Under Engineering for Polar Operations, Logistics, and Research (EPOLAR)
EP-ANT-15-36, "Geophysical Survey of McMurdo Ice Shelf to Determine Current Infrastructure Stability and for Future Planning"

Abstract

Recent surface melting and Antarctic ice-shelf retreat have led to concerns about McMurdo Ice Shelf (MIS) instability, which could threaten research in Antarctica. Researchers at the U.S. Army Cold Regions Research and Engineering Laboratory collected approximately 1300 km of ground-penetrating radar (GPR) profiles over MIS, using frequencies between 40 and 400 MHz, to determine extent, continuity, and depth of the brine and ice-shelf thickness; to map englacial horizons; and to locate any structural features that may suggest shelf instability.

We suggest that brine, sediment-rich ice, and a rough direct coupling attenuates the signal in this region of MIS. Results show no major englacial features that raise concerns for shelf stability; however, two locations are worthy of continued monitoring from an operational and safety perspective. The first location is a prior Antarctic Geological Drilling (ANDRILL) site from 2006; the infrastructure established during ANDRILL operations appears to have actually influenced ice dynamics in the region. The second location is a long-term rift located near the ice shelf–sea ice edge. This study supports prior results that suggest that repeat high-resolution, ground-based GPR is useful for reconstructing ice-shelf history through analysis of imaged englacial and basal structures.

Contents

Figures and Tables

Figures

Tables

Preface

This study was conducted for the National Science Foundation (NSF) through Inter Agency Agreement Number 1564557 under Engineering for Polar Operations, Logistics, and Research (EPOLAR) EP-ANT-15-36, "Geophysical Survey of McMurdo Ice Shelf to Determine Current Infrastructure Stability and for Future Planning." The technical monitor was Margaret Knuth, NSF Office of Polar Programs, Antarctic Infrastructure and Logistics.

The work was performed by the Engineering Resources Branch (CEERD-RZE) and the Terrestrial and Cryospheric Sciences Branch (CEERD-RRG), U.S. Army Engineer Research and Development Center, Cold Regions Research and Engineering Laboratory (ERDC-CRREL), and the Department of Geology, Middlebury College, Middlebury, VT. At the time of publication, Jared Oren was Chief, CEERD-RZE); J. D. Horne was Chief (CEERD-RRG), and Janet Hardy was the program manager for EPOLAR. The Deputy Director of ERDC-CRREL was Dr. Lance Hansen, and the Director was Dr. Robert Davis.

We appreciate Polar Geospatial Center for providing GIS (geographic information system) mapping support and UNAVCO for providing GPS (Global Positioning System) support. We also appreciate Lockheed and associated subcontractors for providing key logistical support, specifically USAP's Ryan Wallace, Baija Sass, Tony Buchannan, Meghan Parks, Bev Walker, and John Loomis.

Dr. Seth Campbell was the principal investigator and wrote the majority of this paper. Dr. Zoe Courville (who contributed the text regarding the ice-core work) and Dr. Sally Shoop were co-investigators. Courville and Campbell conducted the fieldwork with field assistance provided by Stephen Zellerhoff, Marie McLane, Paul Koubek, Jonathan White, Laura Gerwin, Michael Pfalmer, and Ester Babcock, all of the United States Antarctic Program (USAP). Samantha Sinclair and Joel Wilner assisted with data processing, analysis, and writing. Campbell processed all ground-penetrating-radar (GPR) profiles; Courville processed all core samples; and Sinclair, Wilner, and Campbell picked ice-shelf bottom and brine horizons for interpolations.

COL Bryan S. Green was Commander of ERDC, and Dr. Jeffery P. Holland was the Director.

Acronyms and Abbreviations

ANDRILL	Antarctic Geological Drilling
CRREL	Cold Regions Research and Engineering Laboratory
EPOLAR	Engineering for Polar Operations and Logistics
ERDC	Engineer Research and Development Center
GIS	Geographic Information System
GPR	Ground-Penetrating Radar
GPS	Global Positioning System
GSSI	Geophysical Survey System Incorporated
MIS	McMurdo Ice Shelf
MLF	Multiple (Adjustable) Low-Frequency
NIR	Near Infrared
NSF	National Science Foundation
SCS	Surface-Conformable Stratigraphy
SIPRE	Snow Ice and Permafrost Research Establishment
TWTT	Two-Way Travel Time
USAP	U.S. Antarctic Program

1 Introduction

1.1 Background

The McMurdo Ice Shelf (MIS) in West Antarctica has experienced a noteworthy retreat and readvancement over the past 70 years. As recently as 1947, MIS fractured or retreated enough to allow the migration of seal populations to White Island, a landmass 18 km inland from the current ice shelf's front (Gelatt et al. 2010). Other than the migrated seal population, no physical evidence has been found within the ice shelf itself to confirm its retreat or fracturing. However, surface melting and general Antarctic ice-shelf instability has been of scientific concern since the 1960s (Paige 1968; Kovacs and Gow 1975). Recent findings of instability within the West Antarctic Ice Sheet and the surrounding ice shelves (e.g., Joughin et al. 2014; Rignot et al. 2014), when combined with (a) the knowledge of basal crevasse and subglacial water channel impacts on ice stability (Sergienko and Hulbe 2011; Luckman et al. 2012), (b) the documentation of calving (such as Iceberg B-15's break-up event) that could influence the ice pack around MIS (Blue Ribbon Panel 2012), and (c) the recent melting around Pegasus Runway (Shoop et al. 2013), have generated a heightened level of concern for the stability of MIS, from both operational and scientific standpoints. Impacts of ice-shelf failure on up-glacier dynamics are also well known (Scambos et al. 2004). Operationally, the seriousness of this issue was summarized by the Blue Ribbon Panel when its 2012 report indicated that an interruption of MIS runway operations could be considered a "single-point failure" that would jeopardize both the U.S. and New Zealand Antarctic programs.

Kovacs and Gow's (1975) initial ground-penetrating radar (GPR) surveys of MIS near its terminus revealed step discontinuities within the brine layer that were interpreted as evidence of prior large-scale fractures or calving events. Morse and Waddington (1994) imaged similar features within the brine horizon and argued that they were evidence of lateral motion (brine retreat in this instance) in response to ice-front fracture events. Grima et al. (2016) used extensive airborne radar centered at 60 MHz to develop a broad understanding of the brine extent, snow, firn, and ice conditions of MIS. They showed a trend of decreasing snow and firn thickness from Ross Island toward Black Island but an inverse relationship in den-

sity and a glacial-ice ablation area existing toward Black Island. They attributed these thickness and density differences to wind redeposition of accumulation away from Black Island and spatial variations in snowfall, with higher rates near Ross Island. Unfortunately, the low frequency and wide footprint of airborne radar results in low vertical (~5.6–9.5 m) and low horizontal (200–400 m) resolution, respectively, produced a generalization of englacial structures near the MIS terminus. Arcone et al. (2016) used robot-towed GPR to show substantial structural complexities in high resolution that were located upstream of White Island. Their region of interest was part of an approximately 5 km wide by 60 km long shear zone created by a velocity gradient associated with buttressing from Minna Bluff and White Island. The shear zone consists of approximately 150 m of meteoric ice and 20–30 m of stratified marine ice at the ice-shelf base. Buried surface crevasses to 30 m depth and bottom crevasses or rifts, both caused by a combination of tensile and shear stress, are prevalent in profiles collected by Arcone et al. (2016).

1.2 Objective

Interest in the structure of MIS originated from observed surface and basal crevasses up-glacier of MIS. Likewise, an apparently stable surface rift exists near the MIS terminus, which further encouraged research to determine if other englacial features exist that may contribute to future MIS instability. The National Science Foundation, therefore, contracted the U.S. Army Cold Regions Research and Engineering Laboratory (CRREL) to conduct a broad survey of the englacial structure surrounding MIS infrastructure to act as a baseline for comparison against future surveys.

1.3 Scope

This work used a systematic GPR survey of MIS near its terminus to quantify ice thicknesses and the depth and extent of the brine horizon and to locate any structural features within the near-terminus ice shelf (such as large-scale basal fractures, subglacial channels, or brine fractures) that could indicate or affect MIS stability. Detailed methodology is described in Chapter 3.

2 Study Site

MIS within McMurdo Sound is a 1000 km^2 region, which is split from the broader Ross Ice Shelf due to the position of Ross Island (Figure 1). The area is bound by Ross Island's Hut Point, White Island, Black Island, and Brown Peninsula. Glacier ice that flows into McMurdo Sound curls around Minna Bluff and White Island from the south and is buttressed by Ross Island to the north and Hut Point to the west. The ice shelf currently terminates in an arc that starts in front of Scott Base in a north–south orientation. Ice velocities transition from 260–380 m/year within the shear zone upstream of White Island (Courville et al., in prep.; Arcone et al. 2016) to 100–230 m/year between Hut Point and White Island. The slower velocities within McMurdo Sound are attributed to buttressing of Hut Point, which we suggest causes compression and therefore resuturing of rifts created by the velocity gradient up-glacier of White Island and Minna Bluff. Some debris-rich and ablating ice flowing toward the MIS terminus also originates from the Black Island and Brown Peninsula regions.

Figure 1. Landsat image of MIS, showing major features, including White, Black, and Ross Islands; Brown Peninsula; Minna Bluff; Hut Point Peninsula (HP); and general ice flow directions (*black dotted arrows*). Ice-core locations and GPR profiles collected in 2015 are also shown.

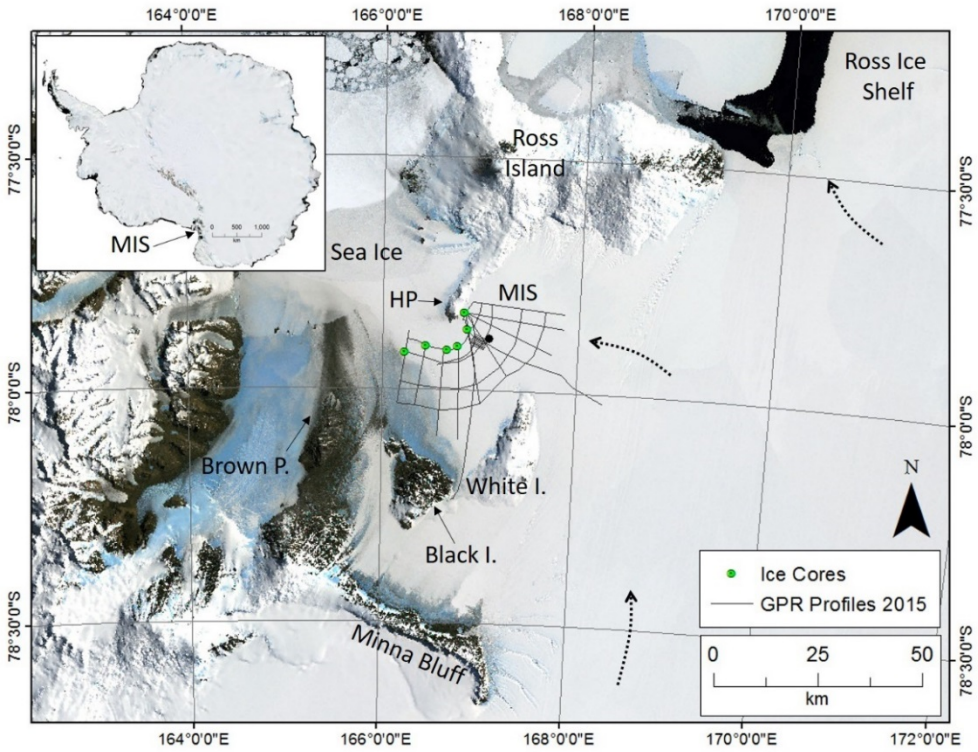

3 Methods

We took measurements with an SIR-4000 GPR control unit coupled with four antennas: a model 3200 MLF (multiple [adjustable] low-frequency) antenna at 40 MHz, a model 3207 at 100 MHz, a model 5106 at 200 MHz, and a model 50400 at 400 MHz. The GPR and antenna units are manufactured by Geophysical Survey Systems Incorporated (GSSI). Eleven approximately 20–45 km long profiles were spaced about 5 km apart and then were collected in a radial pattern and perpendicular to the ice-shelf front toward White Island or Black Island. Seven other profiles were collected parallel to the ice-shelf front and roughly perpendicular to the radial profiles to develop a pseudo 3-dimensional structure map of MIS. In total, about 1300 km of GPR profiles were collected covering the 1000 km^2 area. Profiles were collected via a snowmobile traveling approximately 5–15 km hr^{-1} with 24 scans s^{-1}, resulting in traces being recorded approximately every 10 cm in horizontal distance. Scans were recorded for 1400–2200 ns two-way travel time (TWTT) with 2048 samples per scan; this sampling rate provided 10–17 samples per meter, which is adequate to maintain a smooth waveform given the frequencies used. Profiling was conducted more quickly with the higher-frequency antennas (200 MHz and 400 MHz) due to the shallow depth and strong continuous brine horizon acting as the primary reflector. In contrast, profiles collected to image the ice-shelf bottom (40 MHz and 100 MHz) were collected more slowly at higher sampling rates to ensure stratigraphy was also imaged. Processing of each GPR profile included time-zero correction, bandpass filtering, stacking, and depth calibration.

We initially planned to use 100 MHz and 200 MHz antennas to assess basal ice-shelf conditions; these antennas have about 86 cm and 44 cm vertical resolutions, respectively, based on an the dialectic constant for ice ($\acute{\varepsilon}$) of 3.1 and assuming $\frac{1}{2}$ of the wavelength (γ) is required to distinguish horizons from one another. We planned to use the 400 MHz antenna to assess near-surface features and the brine horizon due to its higher vertical resolution at about 22 cm using the same $\frac{1}{2}\gamma$ assumption. In regions where the highly conductive brine layer infiltrates the MIS, thereby reducing GPR penetration depth (Clough 1973; Kovacs et al. 1982a, 1982b; Morey and Kovacs 1982; Arcone et al. 1994; Arcone 1996), we relied on shallow stratigraphy and brine-layer discontinuities to indicate potential fracture locations. We also attempted to use the 40 MHz antenna (4.3 m γ at $\acute{\varepsilon}$ = 3.1 or

~2.2 m vertical resolution based on $\frac{1}{2}\gamma$) to penetrate the brine horizon and image the ice-shelf bottom near its terminus and transition to sea ice. Profiles were geo-referenced using a Trimble 5700 Rover with a Zephyr Geodetic GPS (Global Positioning System) antenna (1–3 m spatial accuracy). Following Arcone (1996), our interpretation of horizons or reflections within radar profiles, in part, comes from an analysis of the waveform polarity first three half cycles, resulting from interfaces between two materials with $\acute{\varepsilon}$ contrasts. That is, a positive triplet (+ − +) suggests that the deeper layer or target has a higher $\acute{\varepsilon}$ than the overlying layer, and a negative triplet (− + −) suggests that the deeper layer or target has a lower $\acute{\varepsilon}$.

Ground truth and depth calibration of the brine horizon (imaged using GPR) came from six cores drilled near the ice-shelf edge by using a hand-powered SIPRE (Snow Ice and Permafrost Research Establishment) corer with a 7.5 cm diameter, 1 m long core barrel (Table 1; Figure 2). Core lengths ranged between 6 and 15 m, and coring was terminated once the brine horizon was reached. This horizon was typically distinguished immediately by an obviously wet and saline layer within the core. Each core was processed for stratigraphy, density, salinity, and conductivity at 10 cm resolution to confirm that the brine horizon was reached. Stratigraphy was recorded in the field and imaged using a near-infrared (NIR) digital camera (Figure 3). The density was determined gravimetrically by using a digital balance to measure mass and digital calipers to measure the diameter and length of core sections. Cores were bagged, melted, and allowed to reach a temperature equilibrium. Salinity, conductivity, and temperature of each sample at the time of measurement were determined by using a YSI Pro Series salinity/conductivity probe. The probe was rinsed in fresh water between each measurement. Ice-shelf bottom depths in GPR profiles were estimated by using dry ice velocities (v), assuming $\acute{\varepsilon}$ = 3.1; v = 0.169 m ns^{-1}. Common midpoint GPR surveys for depth calibration were not conducted; therefore, we provide TWTT in the discussion of each profile to minimize velocity or depth assumptions.

Table 1. Firn- and ice-core properties.

Core #	Latitude	Longitude	Length (m)	Average Density (g/cm^3)	Brine Layer Depth (m)	Maximum Salinity (ppt)
Core 1	-77.8343	166.8373	15.1	0.67	14.9	9.4
Core 2	-77.8699	166.8679	7.6	0.55	6.4	0.1
Core 3	-77.9071	166.7776	5.4	0.57	4.6	1.8
Core 4	-77.9153	166.6636	6.9	0.60	6.4	21.1
Core 5	-77.9063	166.4499	4.2	0.91	1.4	2.3
Core 6	-77.9203	166.2299	6.2	0.75	5.4	0.7

Figure 2. Stratigraphy and density profiles of shallow firn and ice cores collected from MIS. *Circles* within the density plot denote discrete measured samples in 10 cm intervals, and the *blue band* indicates the brine horizon noted within each core through associated conductivity measurements of each core sample (0.1 ppt resolution). Core logs represent stratigraphy of each core, with dark gray representing pore close-off depth (density ≥ 0.82 g cm^{-3}). High densities at the bottom of the cores are due to unfrozen brine creating a wet, slushy layer in the firn.

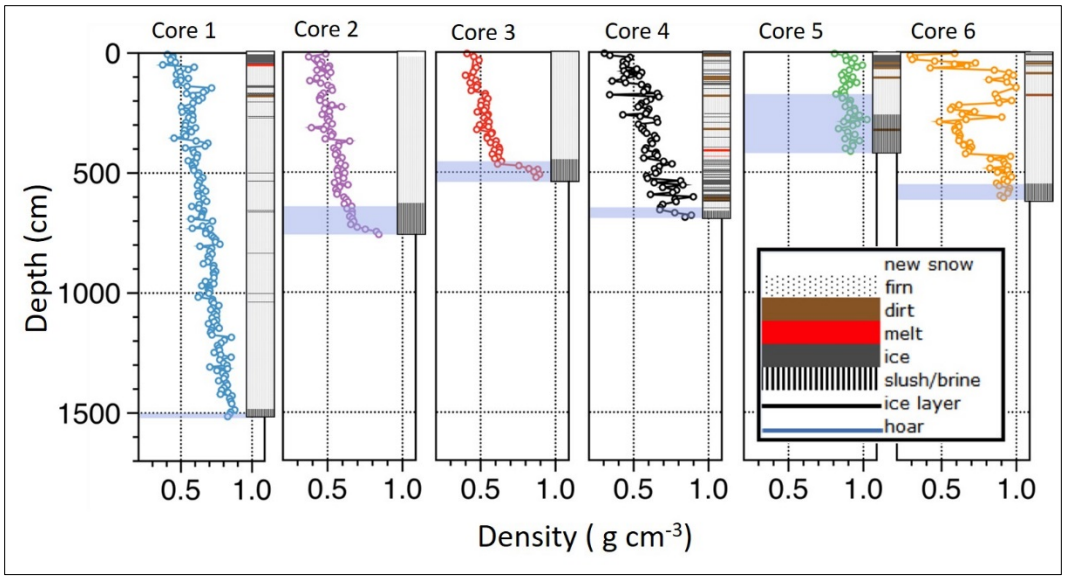

Figure 3. Example of features imaged in shallow ice and firn cores using NIR digital photography.

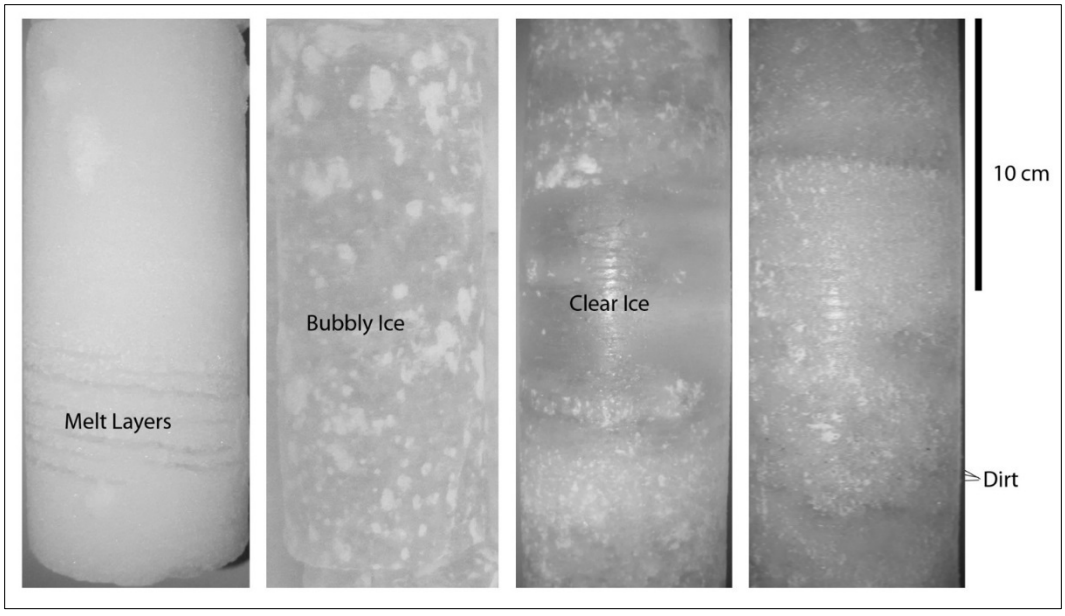

4 Results and Discussion

4.1 Ice and firn cores

Table 1 summarizes the physical properties of the six ice cores, with detailed stratigraphy of the cores illustrated in Figures 2 and 3. Salinity indicated the overall presence of brine, and the maximum salinity recorded is indicative of how deep into the brine layer each core was drilled. Cores 1, 2, and 5 were drilled well into the brine layer while Cores 3 and 4 extended into only the top portion of the brine. Core 5 was drilled in a glacial-ice area that appears to contain a diffuse brine throughout much of the core length. Core 6 also exhibited brine within glacial ice near the bottom of the core. Most of the cores consisted of new snow and firn in the upper several meters with the exception of Core 5, which was drilled into 2 cm of fresh snow and then bare ice (i.e., no firn layer), and Core 6, which contained no snow cover and was drilled in a glacial-ice region. Thin layers of dust, typically consisting of fine particle sizes, were found in all but two of the melted cores (Cores 2 and 3). Core 4 exhibited the most dust-deposition events as indicated by individual layers and bands with the highest concentration of dust. All cores except Cores 2 and 3 also showed indications of melt as either (a) clear, bubble-free ice layers detected within the firn (indicating melt percolation and saturation of firn layers) or (b) very clear melt layers that contain bubbly ice as indicators of melt and refreeze.

4.2 Ice shelf

The 400, 200, and 100 MHz antennas each successfully imaged the ice-shelf bottom to a maximum of 165 m deep (1950 ns TWTT), where the longest profile collected terminates in a region studied and discussed by Arcone et al. (2016) known as the McMurdo shear zone (Figure 4). Only two profiles, both using the 100 MHz antenna, successfully penetrated to the ice-shelf bottom under the brine (Figure 5). Ice thicknesses for these two profiles were highly variable, ranging from 10 to 38 m deep. Up-glacier of brine infiltration, the 100, 200, and 400 MHz antennas each successfully imaged internal stratigraphy, the ice-shelf base, and associated basal shelf fractures (Figure 6). In unmigrated profiles, basal fractures appeared as hyperbolas approximately 20 m above the ice-shelf bottom, suggesting that these fractures extend that far into the ice-shelf base. The hyperbolas' footprints mask the ice-shelf base near the fractures; however, they appear to be consistently about 120–140 m in width (Figure 7). Note

that the dimensions and geophysical signatures of these fractures are similar to subglacial channels; however, the ice flow dynamics of this region are well known and do not support a hypothesis of subglacial channels. Therefore, our interpretation of these fractures is that they represent rifts caused by the velocity gradient near White Island that have been resutured within MIS. Surface expression of the features at the same locations are visible in Figure 4.

Figure 4. Map with Landsat imagery showing ice-shelf thicknesses from GPR profiles collected during this study. *Gray lines* are approximate locations of all GPR profiles collected in the fall of 2015, and the background color is from the Norwegian Polar Institute Quantarctica ice flow velocity dataset. Core sites 1 through 6 are labeled (C1–C6) as are the rifts caused by White Island (e.g., Fig. 5).

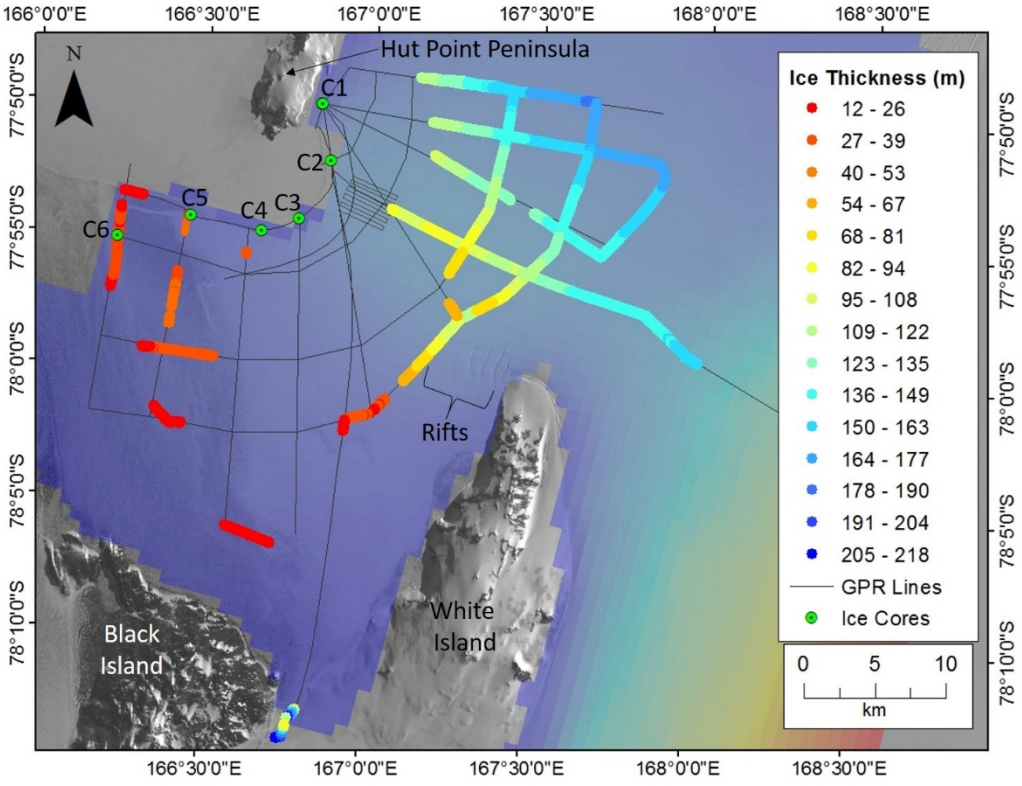

Figure 5. 100 MHz GPR profile showing brine horizon over the ice shelf. Profile was the most distal collected parallel to the ice-shelf terminus (i.e., north to south) in this study. Note the rift that was likely initiated due to buttressing of White Island as ice flowed around the corner, now filled with surface-conformable stratigraphy (see Fig. 4 for location). The figure also shows the actual wave triplet responses for direct coupling, ice over brine, and ice-shelf bottom in the figure profile near 6.5 km distance along the x-axis.

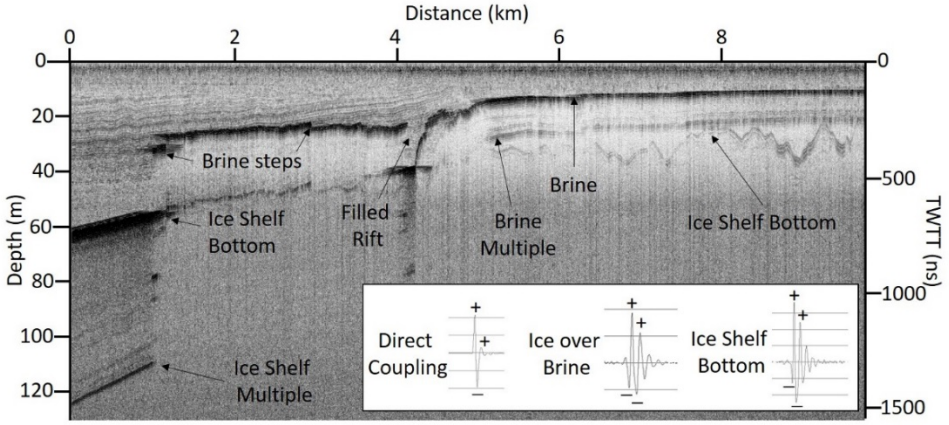

Figure 6. Profile from the shear zone studied by Arcone et al. (2016) to the ice-shelf terminus near Scott Base, showing basal fractures in the ice-shelf bottom, masking of the ice shelf by the brine horizon, and a brine-horizon multiple. Also note the ANDRILL (Antarctic Geological Drilling) site (discussed in the text).

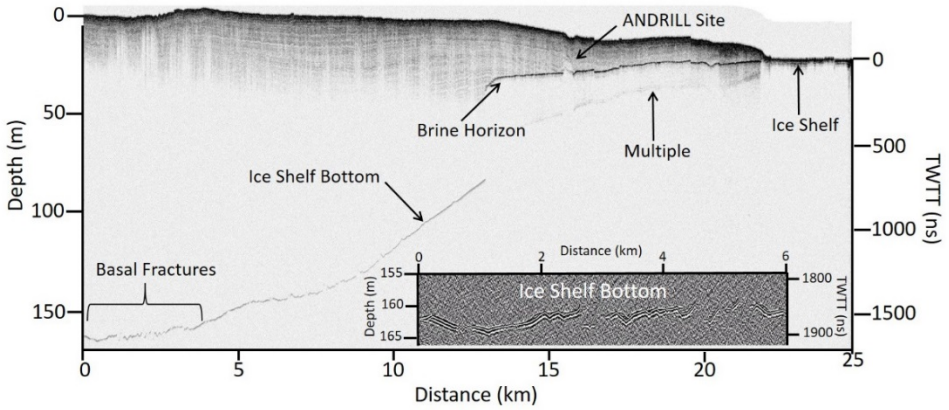

Figure 7. A 200 MHz profile of subglacial fractures located north and slightly downstream of White Island.

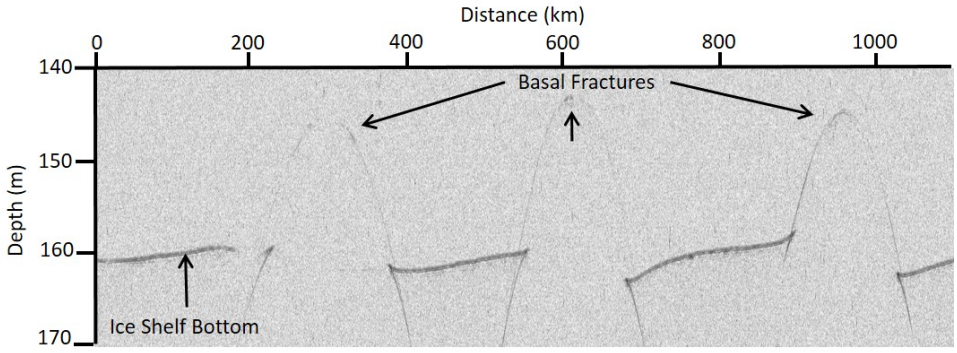

MIS exhibits a marked transition with the convergence of ice originating from near White Island (Figure 6) and ice originating from Black Island and Brown Peninsula (Figure 8a). The convergence of these two flows occurs within the ablation zone of MIS. Ice originating from the Brown Peninsula region shows significant stratification whereas ice originating from between Ross and White Islands shows minimal or diffuse stratification. We interpret the stratified layers within the Brown Peninsula ice to be representative of entrained sediment or dust deposits originating from Black Island, Minna Bluff, or Brown Peninsula. The unconformity between these two ice units is consistent and unmistakable in multiple profiles that crossed into this southern ablation region of MIS.

Two large-scale features exist on the ice shelf that should be monitored for future changes. The first is a 10 km long rift located approximately 1 km upstream of and oriented parallel to the ice-shelf edge. The rift is also located 4 km northwest and downstream of the north threshold of the Pegasus Runway. GPR profiles show a 75–100 m wide discontinuity in the brine horizon at a 24 m depth, a velocity pull-up on either side of the discontinuity, and a lack of stratigraphy within the rift zone as shallow as 5 m in depth, suggesting that seawater cuts across and above the brine horizon, potentially filling a large void where the rift is located (Figure 8b). We interpret this feature to be a bottom fracture that has propagated to become located near the surface.

GPR profiles of a second site, located 1–2 km up-glacier of Pegasus Road and along the South Pole traverse route, shows similar features to the rift. A GPR grid revealed that this oblate feature is 600 × 1000 m in dimension and depressed from the surrounding topography by roughly 5 m. The structure is capped by a hyperbolic reflection at a 10 m depth, lacks any fine firn stratigraphy within, and truncates stratigraphic horizons to the north and south between 10 and 20 m in depth (Figure 9). The bottom of this feature is defined by the surrounding brine horizon, which is either discontinuous across the feature or reduced in reflection return power within the feature.

Figure 8. A 100 MHz GPR profile with inset map (*top*) and zoom of buried features (*bottom*). The *upper* figure shows dust-rich ice originating from Black Island and Brown Peninsula regions under MIS ice with a rift located near the ice-shelf front. Inset map shows the location of the GPR profile on the ice shelf, which also corresponds with the location of C6 in Fig. 5. The *lower* figure is a zoom of the dust-rich ice and MIS contact, the velocity uplift near the rift, and ice-shelf bottom horizon.

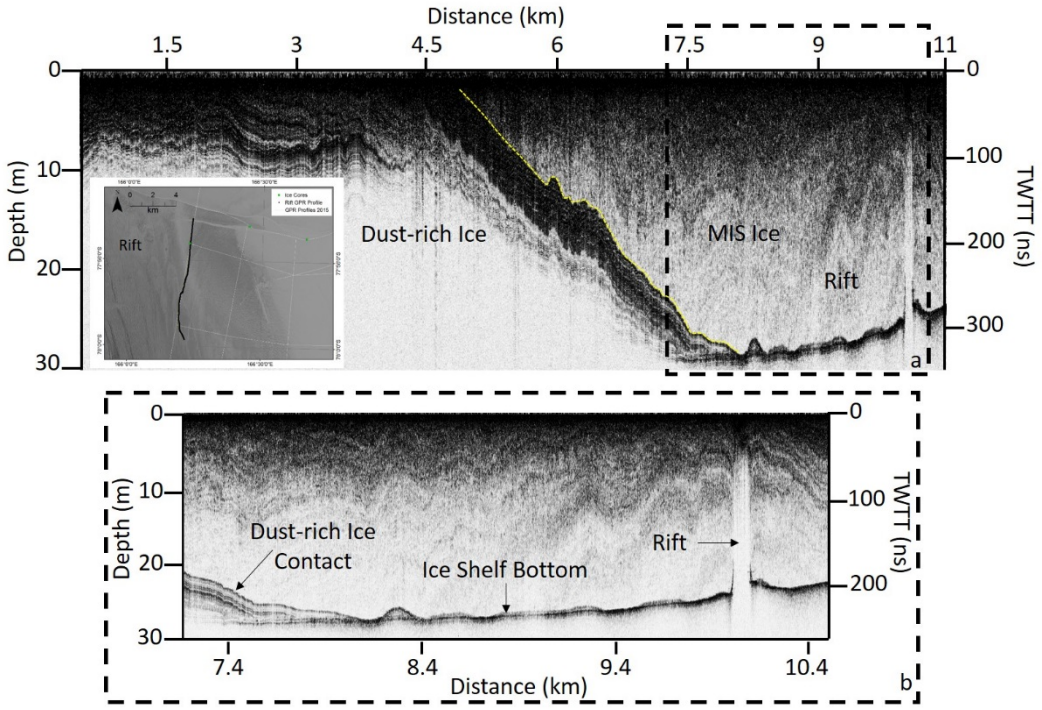

Figure 9. A 400 MHz GPR profile showing the impact of the ANDRILL drilling site on MIS. Note the unconformity between the SCS and the ANDRILL site, which has only two prominent horizons—likely caused by the influence of hot-water drilling activities. Also, note the significant folding located down-glacier of ANDRILL, which reaches to within 5 m of the ice-shelf surface.

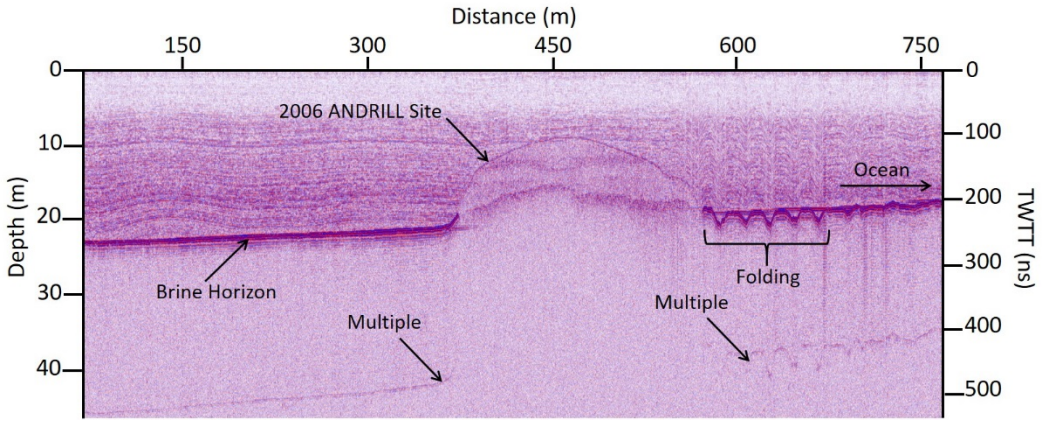

We interpret this feature as the remains of the prior ANDRILL deep sediment drilling site established in 2006, based on available prior ANDRILL

coordinates, local ice flow velocities placing the drill site now in this location, and the estimated footprint of the ANDRILL establishment. Note that ANDRILL appears to have influenced the glacier flow significantly enough to act as a pinning point on the shelf by reducing flexure up-glacier but causing folding of the ice immediately down-glacier of the borehole site. We propose that hot-water drilling to maintain an open hole at ANDRILL acted similarly to surface melt water percolating within a temperate snowpack; that is, stratigraphic horizons in the GPR record caused by chemistry or density contrasts were disturbed from the introduced water, thereby diffusing horizons and associated stratigraphy within radar profiles. The result is an apparent unconformity between the surface-conformable stratigraphy (SCS) surrounding ANDRILL and a lack of finer stratigraphy within the ANDRILL region. A few faint, yet diffuse, horizons are visible within the ANDRILL site, and we interpret them to be the thick, saline brine horizon and perhaps a shallower, thick, dusty horizon that resisted diffusion from the introduced hot water.

4.3 Brine

Previous studies have suggested various mechanisms for ice-shelf brine infiltration, including upward percolation of seawater through basal tensile cracks, upward diffusion at ice-crystal boundaries, and lateral infiltration at the shelf front (Kovacs and Gow 1975; Kovacs et al. 1982a). Periodic lateral infiltration at the ice margin is considered the primary mechanism for brine infiltration into MIS (Kovacs et al. 1982b). Evidence in support of this mechanism comes from the observation of large fractures, as manifested by offsets, within the MIS brine horizon that represent former wave-like intrusions of seawater that originated at the ice front after a large calving event (Kovacs et al. 1982a; Cragin et al. 1983). In describing the termination of brine infiltration, Kovacs et al. (1982b) invoke an equation that was introduced by Thomas (1975) for brine flow velocity u:

$$u = \frac{B_0}{\eta} \frac{\partial p}{\partial x} \tag{1}$$

where

B_0 = the specific permeability of firn,
η = the dynamic viscosity of brine fluid, and
$\partial p/\partial x$ ~ the pressure gradient over the brine layer.

Eq. (1) shows that brine flow velocity is directly proportional to the specific permeability of firn; hence, brine infiltration terminates when firn permeability is zero. This impermeability is reached at the firn/ice transition zone when firn density reaches 0.82 mg/m^3 (Kovacs and Gow 1975). However, evidence of slow, continued brine migration has been observed in MIS, deeper than the firn/ice transition zone (Kovacs et al. 1982a). In this region, concentrated brine continues to gradually percolate inland into deeper and warmer sections of the ice shelf through the dissolution of the surrounding ice.

The MIS brine horizon extends over 700 km^2 in area and is constrained by White and Black Islands to the south and by Ross Island and McMurdo Sound to the north (Figure 10). Our results show that the horizon penetrates nearly 20 km up-glacier and ranges in depth between about 5 to 52 m (~70 to 460 ns TWTT) from the ice-shelf front moving up-glacier. Other studies show similar results (Heine 1968; Kovacs and Gow 1975; Kovacs et al. 1982a). Profiles that were collected parallel to the ice-shelf front reveal that the horizon undulates up to 10 m in depth over relatively short distances (~100–200 m).

Several discontinuities or fractures exist within the brine that are similar to those imaged in prior studies (e.g., Kovacs and Gow 1975; Kovacs et al. 1982a; Kovacs et al. 1982b; Morse and Waddington 1994). These “steps” (as termed by prior authors) vary in size from submeter to several meters tall and have been observed within the brine horizon and at the most distal up-glacier extent of the horizon. Small, closely spaced steps typically characterize the inland termination of a brine horizon (e.g., Figure 5) while larger steps may depict former calving events, fracturing, or rifting (Kovacs et al. 1982a). We propose that the lateral extent and depth of brine within the shelf, along with stratigraphic information determined by GPR, could provide a testable model of ice-shelf density structure, permeability, and brine migration processes.

Figure 10. Map with Landsat imagery, showing the depth to brine from GPR profiles collected during this study. *Gray lines* are approximate locations of all GPR profiles collected in fall 2015, and background color is from the Quantarctica ice flow velocity dataset. Core sites 1 through 6 are also labeled (C1–C6).

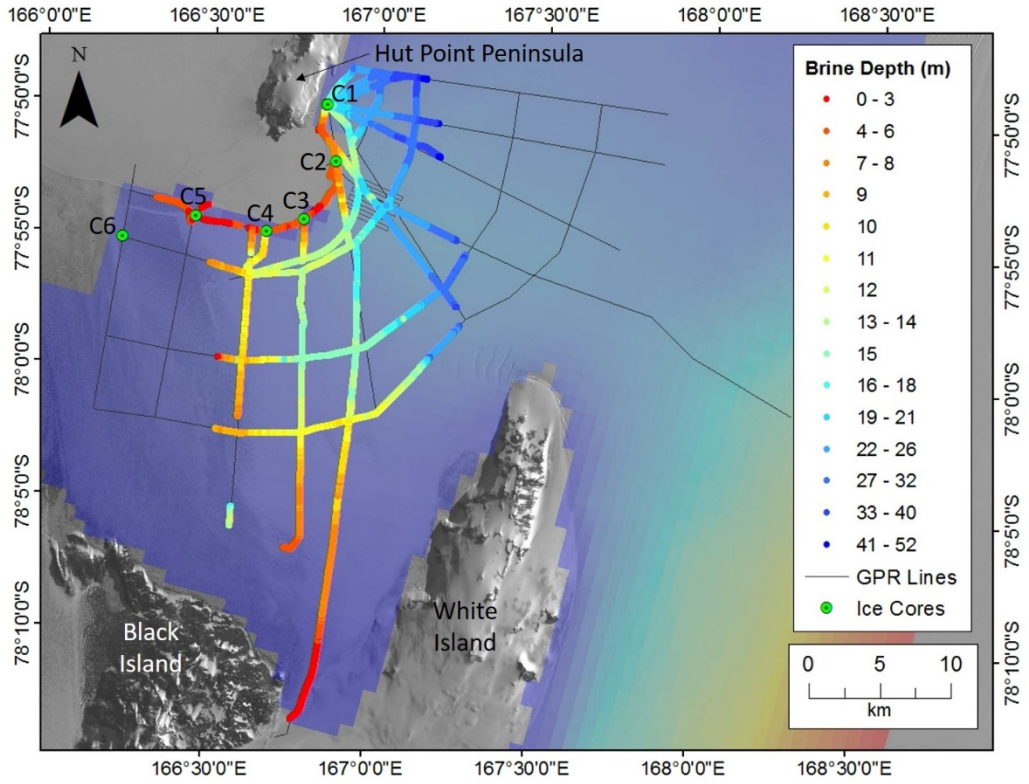

4.4 Englacial structure

GPR profiles reveal a combination of SCS and complex englacial structures or unconformities across the ice shelf. The 400, 200, and 100 MHz antennas displayed maximum thicknesses of SCS to 40, 50, and 80 m depth, respectively. Stratigraphic units over the brine thicken from Pegasus Runway toward Ross Island (north) (right to left in Figure 11); immediately south of Pegasus Runway, the snow and firn transitions to a glacial-ice ablation surface that persists to the edge of Black Island. This finding corresponds well with the higher accumulation rates near Ross Island relative to White Island, as noted by Grima et al. (2016). We attribute thicker SCS toward Ross Island in large part to katabatic winds originating inland that blow snow past the White Island region. These winds also scour the glacial-ice area and redeposit snow near Ross Island because it acts as a natural topographic block (e.g., Seefeldt et al. 2003). Profiles collected perpendicular to the shelf edge also reveal gradual thickening of the snow and firn above the brine in a direction distal to the ice-shelf front (e.g., Figure 6). Most profiles show that the brine truncates or crosscuts numerous

stratigraphic horizons, which suggests that the brine was formed after the horizons and more importantly that the porous firn structure acts as little hindrance to lateral brine infiltration.

Figure 11. Profile oriented north to south and parallel to the ice-shelf front showing the significant thinning of SCS toward the south.

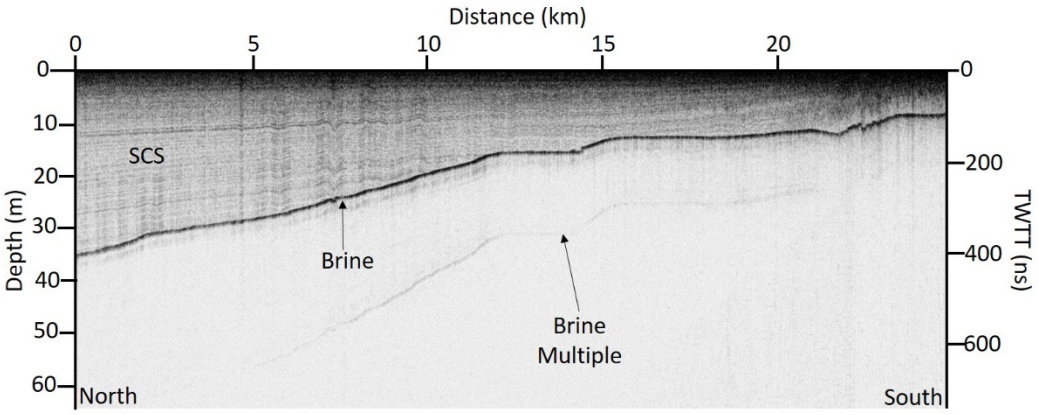

Near the transition zone (named for the transition from sea ice to land by Scott Base), a GPR profile collected slightly oblique to and across the ice-shelf–sea-ice edge (Figure 12, a to a′) reveals a distinct series of synclinal and anticlinal folds within the englacial structure down to a 15 m depth and extending approximately 2 km up-glacier (Figure 13). Fold dips are steeper at depth and appear as crosscut unconformities at the surface. These folds result from compression as the ice shelf flows around White Island and impacts Hut Point Peninsula on Ross Island. Valley glacier ice flowing off Hut Point Peninsula also likely influences the ice shelf as the glacier ice also flows toward the ice-shelf edge. We interpret the synclinal folds to be filled with winter snow accumulation that likely melts each late-summer season, creating the unconformity at the surface. Melt ponds form each year in the synclinal depressions to the north of this GPR profile but still within the transition zone (Figure 12), suggesting that much of the folded structure in this area consists of impermeable glacial ice. However, the brine horizon can be traced from roughly 0 to 180 ns TWTT in depth originating at the ice-shelf–sea-ice transition (~0–17 m where $\acute{\varepsilon} = 2.2$). The brine creates an unconformity relative to the folded stratigraphy, again, suggesting that the folds are both permeable (i.e., likely firn) and that it is not a hindrance to lateral brine infiltration. It is also possible that the brine in this area diffuses through layers as suggested by Kovacs et al. (1982a). Regardless of the mechanism for brine infiltration, it is obvious—

based on the GPR and visible observations—that the density and stratigraphy of the transition zone are intricate and would therefore require a more detailed survey to determine the nature of these structural complexities.

Figure 12. Aerial photo showing the transition zone located near Scott Base with major features labeled including approximate ice flow directions (*arrows*). Note the melt ponds situated within the synclinal folds of the transition zone and the approximate location of Fig. 13 denoted by a and a′. (Photo courtesy of Ben Roth.)

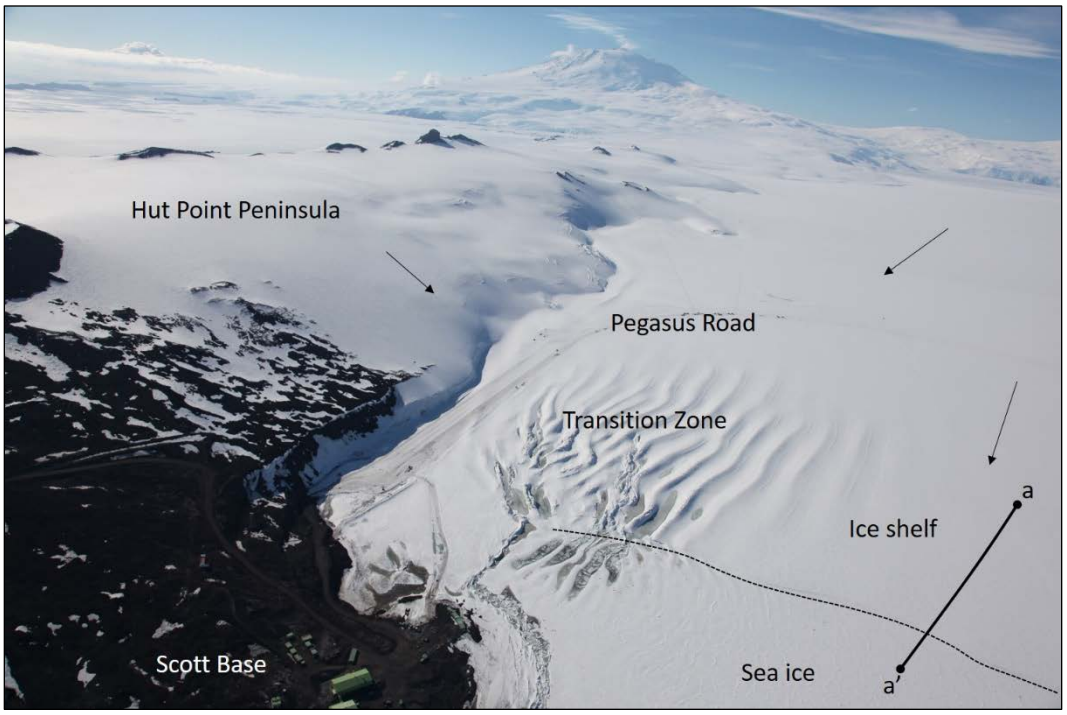

Figure 13. A 100 MHz GPR profile showing folds near the transition zone that are crosscut by the brine horizon. Also, note the approximate location of the winter accumulation filling in the synclinal portion of each fold.

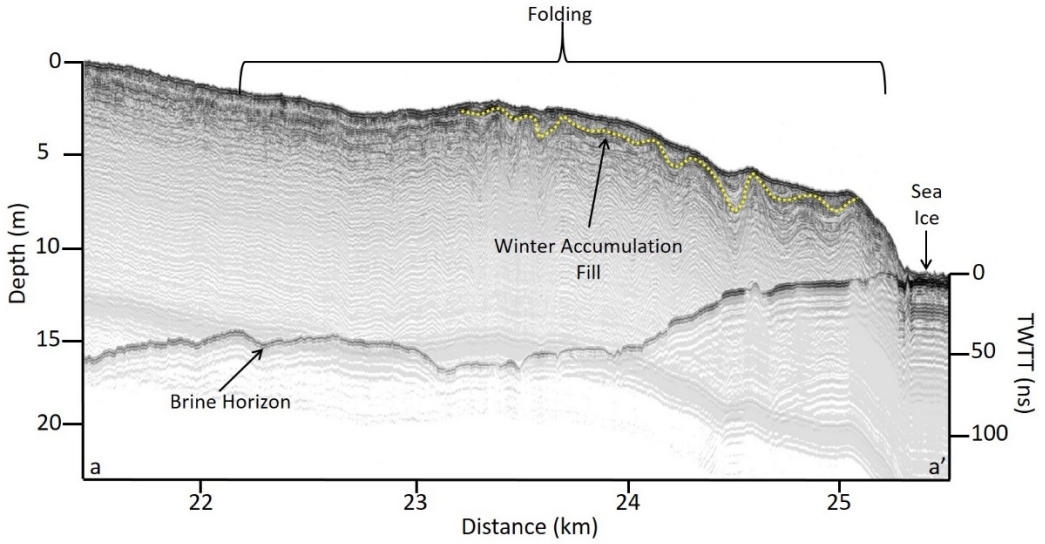

4.5 Dynamic signals: fractures, suture blocks, folds, and rifts

Ice-shelf fracturing and resuturing of these fractured blocks have occurred from expansion and compression as ice flows around White Island into McMurdo Sound. These features are obvious both in satellite imagery and also in GPR profiles collected near White Island. Within an ice shelf, basal crevasses (e.g., Figure 7) can propagate up through the ice by gradual upward penetration of seawater and can theoretically reach up to 78% of the thickness of the ice shelf (Weertman 1980). Surface crevasses (e.g., Figure 5) can propagate downward in regions where a sufficient flux of meltwater exists on the surface of the ice sheet (Fastook and Schmidt 1982). Basal and surface crevasses located in close proximity to one another can become conjoined and form full fractures that extend the entire thickness of the ice shelf. Full fractures could significantly destabilize MIS and put it at risk of increased calving activity and eventual breakup. Fortunately, no continuous feature exists within the ice-shelf proper to suggest any instability. Likewise, surface crevasses appear stable based on SCS located within all major surface fractures noted in GPR profiles; and basal fractures appear to propagate only 10%–15% of the total ice-shelf thickness, suggesting that seawater has not yet significantly influenced these fractures or that ice-shelf compression plays the dominant role in these regions.

The folds that occur down-glacier of the ANDRILL site (Figure 9) suggest how little force is required at the surface to potentially alter ice-shelf dynamics. Although apparently stable for the time being, the transition zone folding and structural complexities will likely be exacerbated if surface melting increases notably during the coming years. Finally, future observations of any changes occurring in (a) the transition zone, (b) the ice-shelf rift near the front of MIS, and (c) the known subglacial suture zones and basal fractures situated north and west of White Island may provide direct evidence of glacial instability.

5 Conclusions and Recommendations

GPR surveys were conducted to successfully map the base and englacial structure of MIS, including ice-shelf thickness; the extent, depth, and continuity of the brine horizon; and englacial stratigraphy, unconformities, or discontinuities. In most places, the brine blocked radar signal penetration, prohibiting imaging of the bottom of the ice shelf, except for profiles most distal to the ice-shelf front. This radar signal suggests a salinity gradient of the brine that supports earlier studies. Several basal ice-shelf fractures and brine discontinuities exist, which can mostly be explained by ice flow dynamics. However, two particular brine discontinuities reveal potential salt water infiltration to within 5–10 m of the surface, one of which is a known rift at the ice-shelf front, and the second appears to be remains of the ANDRILL site. Future high-spatial-resolution radar studies and ice coring should be completed at these two locations to confirm the internal structure, orientation, and extent of these features. These studies may address whether the features represent potential impacts to the long-term stability of MIS. This study acts as a baseline for future site-specific research and for planning of logistical infrastructure to be sited on McMurdo Ice Shelf in the future.

References

Arcone, S. A. 1996. High Resolution of Glacial Ice Stratigraphy: A Ground Penetrating Radar Study of Pegasus Runway, McMurdo Station, Antarctica. *Geophysics* 61 (6): 1653–1663.

Arcone, S. A., A. J. Delaney, and W. Tobiasson. 1994. *Subsurface Radar Investigations at the Pegasus Glacial-Ice Runway and Williams Field, McMurdo Station, Antarctica*. Report 94-12. Hanover, NH: U.S. Army Cold Regions Research and Engineering Laboratory.

Arcone, S. A., J. H. Lever, L. E. Ray, B. S. Walker, G. Hamilton, and L. Kaluzienski. 2016. Ground-Penetrating Radar Profiles of the McMurdo Shear Zone, Antarctica, Acquired with an Unmanned Rover: Interpretation of Crevasses, Fractures, and Folds within Firn and Marine Ice. *Geophysics* 81 (1): WA21–WA34.

Blue Ribbon Panel. 2012. *More and Better Science in Antarctica Through Increased Logistical Effectiveness*. Report of the U.S. Antarctic Program Blue Ribbon Panel. Washington, DC: National Science Foundation.

Clough, J. W. 1973. Radio Echo Sounding: Brine Percolation Layer. *Journal of Glaciology* 12 (64): 141–143.

Courville, Z., B. Walker, and J. Weale. Condition of the McMurdo Shear Zone. In prep. *Cold Regions Science and Technology*.

Cragin, J. H., A. J. Gow, and A. Kovacs. 1983. *Chemical Fractionation of Brine in the McMurdo Ice Shelf, Antarctica*. Report 83-6. Hanover, NH: U.S. Army Cold Regions Research and Engineering Laboratory.

Fastook, J. L., and W. F. Schmidt. 1982. Finite Element Analysis of Calving from Ice Fronts. *Annals of Glaciology* 3:103–106.

Gelatt, T. S., C. S. Davis, I. Stirling, D. B. Siniff, C. Strobeck, and I. Delisle. 2010. History and Fate of a Small Isolated Population of Weddell Seals at White Island, Antarctica. *Conservation Genetics* 11 (3): 721–735.

Grima, C., J. S. Greenbaum, E. J. Lopez Garcia, K. M. Soderlund, A. Rosales, D. D. Blankenship, and D. A. Young. 2016. Radar Detection of the Brine Extent at McMurdo Ice Shelf, Antarctica, and its Control by Snow Accumulation. *Geophysical Research Letters* 43 (13): 7011–7018.

Heine, A. J. 1968. Brine in the McMurdo Ice Shelf, Antarctica. *New Zealand Journal of Geology and Geophysics* 11 (4): 829–839.

Joughin, I., B. E. Smith, and B. Medley. 2014. Marine Ice Sheet Collapse Potentially Underway for Thwaites Glacier Basin, West Antarctica. *Science* 344 (6185): 735–738.

Kovacs, A., and A. J. Gow. 1975. Brine Infiltration in the McMurdo Ice Shelf, McMurdo Sound, Antarctica. *Journal of Geophysical Research* 80 (15): 1957–1961.

Kovacs, A., A. J. Gow, and J. H. Cragin. 1982a. The Brine Zone in the McMurdo Ice Shelf, Antarctica. *Annals of Glaciology* 3 (1): 166–171.

Kovacs A., A. J. Gow, J. H. Cragin, and R. M. Morey. 1982b. *The Brine Zone in the McMurdo Ice Shelf, Antarctica*. Report 82-39. Hanover, NH: U.S. Army Cold Regions Research and Engineering Laboratory.

Luckman, A., D. Jansen, B. Kulessa, E. C. King, P. Sammonds, and D.I. Benn. 2012. Basal Crevasses in Larsen C Ice Shelf and Implications for Their Global Abundance. *Cryosphere* 6 (1): 113–123.

Morey, R. M., and A. Kovacs. 1982. *The Effects of Conductivity on High-Resolution Impulse Radar Sounding, Ross Ice Shelf, Antarctica*. CRREL Report 82-42. Hanover, NH: U.S. Army Cold Regions Research and Engineering Laboratory.

Morse, D. L., and E. D. Waddington. 1994. Recent Survey of Brine Infiltration in McMurdo Ice Shelf, Antarctica. *Annals of Glaciol*ogy 20 (1): 215–218.

Paige, R. A. 1968. Sub-Surface Melt Pools in the McMurdo Ice Shelf, Antarctica. *Journal of Glaciol*ogy 7 (51): 511–516.

Rignot, E., J. Mouginot, M. Morlighem, H. Seroussi, and B. Scheuchl. 2014. Widespread Rapid Grounding Line Retreat of Pine Island, Thwaites, Smith, and Kohler Glaciers, West Antarctica, from 1992 to 2011. *Geophysical Research Letters* 41:3502–3509.

Scambos, T. A., J. A. Bohlander, C. A. Shuman, and P. Skvarca. 2004. Glacier Acceleration and Thinning after Ice Shelf Collapse in the Larsen B Embayment, Antarctica. *Geophysical Research Letters* 31 (18): L18402.

Seefeldt, M. W., G. J. Tripoli, and C. R. Stearns. 2003. A High-Resolution Numerical Simulation of the Wind Flow in the Ross Island Region, Antarctica. *Monthly Weather Review* 131:435–458.

Sergienko, O. V., and C. L. Hulbe. 2011. "Sticky Spots" and Subglacial Lakes Under Ice Streams of the Siple Coast, Antarctica. *Annals of Glaciology* 52 (58): 18–22.

Shoop, S., M. Knuth, and W. Wieder. 2013. Measuring Vehicle Impacts on Snow Roads. *Journal of Terramechanics* 50 (1): 63–71.

Thomas, R. H. 1975. Liquid Brine in Ice Shelves. *Journal of Glaciol*ogy 14 (70): 125–136.

Weertman, J. 1980. Bottom Crevasses. *Journal of Glaciol*ogy 25 (91): 185–188.

REPORT DOCUMENTATION PAGE

Form Approved
OMB No. 0704-0188

1. REPORT DATE *(DD-MM-YYYY)*	**2. REPORT TYPE**	**3. DATES COVERED** *(From - To)*
January 2017	Technical Report/Final	

4. TITLE AND SUBTITLE

Geophysical Survey of McMurdo Ice Shelf to Determine Infrastructure Stability and for Future Planning

5a. CONTRACT NUMBER

5b. GRANT NUMBER

5c. PROGRAM ELEMENT NUMBER

6. AUTHOR(S)

Seth Campbell, Zoe Courville, Samantha Sinclair, and Joel Wilner

5d. PROJECT NUMBER

5e. TASK NUMBER
EP-ANT-15-36

5f. WORK UNIT NUMBER

7. PERFORMING ORGANIZATION NAME(S) AND ADDRESS(ES)

U.S. Army Engineer Research and Development Center (ERDC)
Cold Regions Research and Engineering Laboratory (CRREL)
72 Lyme Road
Hanover, NH 03755-1290

8. PERFORMING ORGANIZATION REPORT NUMBER

ERDC/CRREL TR-17-2

9. SPONSORING / MONITORING AGENCY NAME(S) AND ADDRESS(ES)
National Science Foundation, Office of Polar Programs
Antarctic Infrastructure and Logistics
Arlington, VA 22230

10. SPONSOR/MONITOR'S ACRONYM(S)
NSF

11. SPONSOR/MONITOR'S REPORT NUMBER(S)

12. DISTRIBUTION / AVAILABILITY STATEMENT
Approved for public release; distribution is unlimited.

13. SUPPLEMENTARY NOTES

Engineering for Polar Operations, Logistics, and Research (EPOLAR)

14. ABSTRACT

Recent surface melting and Antarctic ice-shelf retreat have led to concerns about McMurdo Ice Shelf (MIS) instability, which could threaten research in Antarctica. Researchers at the U.S. Army Cold Regions Research and Engineering Laboratory collected approximately 1300 km of ground-penetrating radar (GPR) profiles over MIS, using frequencies between 40 and 400 MHz, to determine extent, continuity, and depth of the brine and ice-shelf thickness; to map englacial horizons; and to locate any structural features that may suggest shelf instability.

We suggest that brine, sediment-rich ice, and a rough direct coupling attenuates the signal in this region of MIS. Results show no major englacial features that raise concerns for shelf stability; however, two locations are worthy of continued monitoring from an operational and safety perspective. The first location is a prior Antarctic Geological Drilling (ANDRILL) site from 2006; the infrastructure established during ANDRILL operations appears to have actually influenced ice dynamics in the region. The second location is a long-term rift located near the ice shelf–sea ice edge. This study supports prior results that suggest that repeat high-resolution, ground-based GPR is useful for reconstructing ice-shelf history through analysis of imaged englacial and basal structures.

15. SUBJECT TERMS
Brine, EPOLAR, Geophysical surveys , Glacial stratigraphy, Glacier–ocean interaction, Glaciology, GPR, Ground penetrating radar, McMurdo Ice Shelf (Antarctica), NSF, Snow accumulation

16. SECURITY CLASSIFICATION OF:			**17. LIMITATION OF ABSTRACT**	**18. NUMBER OF PAGES**	**19a. NAME OF RESPONSIBLE PERSON**
a. REPORT	**b. ABSTRACT**	**c. THIS PAGE**			**19b. TELEPHONE NUMBER** *(include area code)*
Unclassified	Unclassified	Unclassified	SAR	31	